

# Numerical Determination of the Local Ordering of $\text{PbMg}_{1/3}\text{Nb}_{2/3}\text{O}_3$ (PMN) from High Resolution Electron Microscopy Images

C. Boulesteix,\* F. Varnier,† A. Llebaria,‡ and E. Husson§

\*LMEA/MATOP-CNRS. Faculté des Sciences de St. Jérôme, Av. Normandie-Nièmen F-13397 Marseille Cédex 30, France; †Lab. des Interactions Photons Matière. Faculté des Sciences de St. Jérôme, Av. Normandie-Nièmen F-13397 Marseille Cédex 30, France;

‡Lab. d'Astronomie Spatiale. Traverse du siphon F-13012 Marseille, France; and §CRPHT/CNRS et Université d'Orléans, F-45071 Orléans Cédex 02

Received December 15, 1992; in revised form April 23, 1993; accepted April 28, 1993

High Resolution Electron Microscopy (HREM) images of PMN ( $\text{PbMg}_{1/3}\text{Nb}_{2/3}\text{O}_3$ ) taken along a  $\langle 110 \rangle$  axis of the cubic (perovskite) structure show that ordered regions of the  $\{111\}$  type exist which correspond to  $AB'_{1/2}B''_{1/2}\text{O}_3$  composition. Wavy fringes in the  $\{111\}$  plane directions reveal some imperfect ordering. A numerical treatment of the HREM images was performed in order to determine both position and size of perfectly ordered regions. After a test experiment, this method shows that (i) ordered regions consist of clusters about 2 nm in diameter regularly spread inside the crystal, (ii) the distance between the centers of neighboring clusters is about 2.5 nm. The regular arrangement of these clusters is due to their composition which differs from the mean composition. The composition of disordered regions is close to  $\text{PbMg}_{1/4}\text{Nb}_{3/4}\text{O}_3$ . In this model some local electrical charge equilibrium could be obtained, at least partly, by oxygen and metal-atom vacancies. © 1994 Academic Press, Inc.

## INTRODUCTION

$\text{PbMg}_{1/3}\text{Nb}_{2/3}\text{O}_3$  (PMN) is the perovskite-structure "relaxor" material that has been the most deeply studied, as much for its technical as for its basic scientific interest (1–6). This compound presents in the cubic (perovskite) structure ordered domains (7, 8) similar to those observed in various other relaxors such as  $\text{PbSc}_{1/2}\text{Ta}_{1/2}\text{O}_3$  (PST) which very easily shows a high degree of ordering (9–12) or  $\text{PbSc}_{1/2}\text{Nb}_{1/2}\text{O}_3$  (PSN) which also shows ordering but to a lower extent (12) and with smaller ordered regions. In the latter two cases the ordering is due to some alternation of Sc and Ta (or Nb) planes in the direction parallel to the  $\{111\}$  planes, giving rise to an ordered perovskite cubic structure where the ordered unit cell parameter is twice as large as that of the disordered structure. We shall refer to this ordering as being of the  $\{111\}$  type. Some other types of ordering may sometimes be detected in these compounds but they are always limited to small areas and will not be considered here. In the case of PMN, the  $\{111\}$  ordering clearly appears on high resolution elec-

tron microscopy (HREM) images (7, 13–15). Since such ordering can exist only in compounds of the  $\text{Pb}B'_{1/2}B''_{1/2}\text{O}_3$  composition, in PMN ordered domains should be of the  $\text{PbMg}_{1/2}\text{Nb}_{1/2}\text{O}_3$  composition (Mg-rich regions) while disordered domains are Mg-poor (or Nb-rich) regions so that the mean composition would be the nominal one:  $\text{PbMg}_{1/3}\text{Nb}_{2/3}\text{O}_3$ . This phenomenon naturally would limit the size of ordered regions, confining them to a cluster configuration. In this paper we support this point of view by using a numerical method which provides the mean size of ordered domains and the mean distance between them.

It should be noted that the 111 diffraction spots of the ordered perovskite structure are visible in the ordered regions while they are forbidden in the unordered regions. Dark field images on these diffraction spots could give the same results as those we obtain from the HREM images (16). However, the dark-field technique makes it possible to visualize only domains larger than about 3 nm in diameter, while domains much smaller than 3 nm in diameter can be seen when using the technique we propose here. This technique will prove useful since, as we shall see, in the case of PMN, domains smaller than 3 nm in diameter are frequently encountered.

## HREM IMAGES

The  $\{111\}$  type ordering (i.e., one  $\{111\}$  plane of  $B'$  type cations and one  $\{111\}$  plane of  $B''$  type cations in a  $\text{Pb}B'_{1/2}B''_{1/2}\text{O}_3$  perovskite structure) was previously studied in detail (17). The ordering is visible when the electron beam is parallel to a  $\langle 110 \rangle$  axis of the structure ( $\langle 100 \rangle$  zone axis pattern or  $\langle 110 \rangle$  ZAP). Roughly the disordered structure gives HREM images appearing as fringes parallel to the (001) plane direction while the ordered structure gives a regular array of points (white in the best conditions of visibility) with a pseudosixfold symmetry. This situation is visible in Fig. 1 for the case of PMN and in Fig. 3a for the case of PST where large ordered regions are

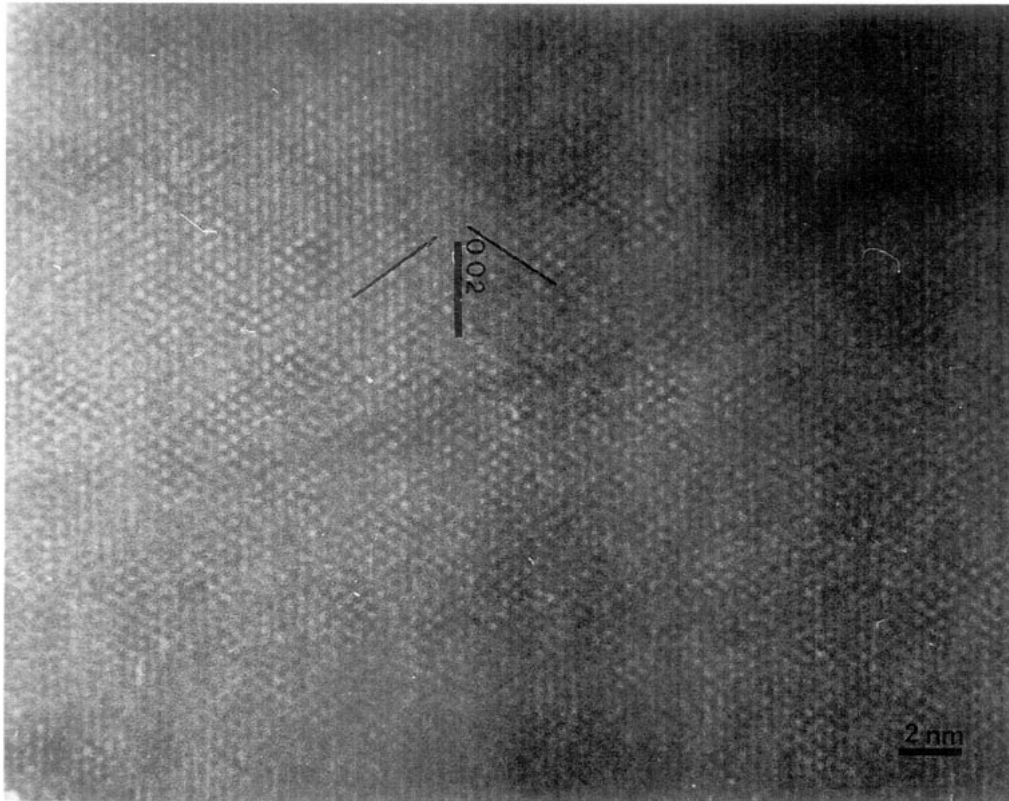


FIG. 1. HREM image of PMN showing ordered and disordered regions. The 002 fringes direction is indicated by a heavy line, the 111 type wavy fringes direction is indicated by a fine line.

neighboring disordered ones with a well defined interface (generally a  $\{111\}$  or the (001) plane). The difference between white spots and fringes being that the 111 (and  $\bar{1}\bar{1}\bar{1}$ ) and  $11\bar{1}$  (and  $\bar{1}\bar{1}1$ ) diffraction spots of the ordered structure (Fig. 2) do not appear when the structure is not ordered. In the case of fringes the HREM image is mainly due to the (002) fringes and in the case of white dots to a composition of (111), ( $11\bar{1}$ ) and (002) fringes. Ordered

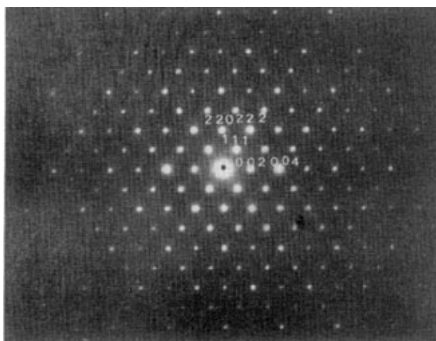


FIG. 2. Electron diffraction pattern for a  $\langle 110 \rangle$  zone axis pattern in an ordered region of PST. Diffraction spots are indexed in the ordered structure.

PMN HREM images are similar to ordered PST but exhibit wavy fringes in the (111) and ( $11\bar{1}$ ) plane directions. This clearly shows that, if ordered domains are spread over very large regions (nearly everywhere in the crystal), the ordering is far from being perfect. As a matter of fact, ordered domains exist everywhere in the crystal but they are separated by disordered or nearly disordered regions. One special point is very important to observe on the HREM images of PMN: the HREM image is visible only close to the edges of crystals. This means that it appears only in thin regions (probably about 5 nm thick) where ordered regions have a little opportunity to overlap in the direction of observation. This would probably smear out the HREM image. Then, if perfectly ordered and disordered regions can be separated, the mean size of the ordered regions and the mean distance between their centers will be determined.

#### PRINCIPLE OF THE IMAGE COMPUTATION

HREM images of ordered regions of PST or of PMN appear as an array of white dots (7, 11, 17, 18). Their Fourier transform yields a diffraction pattern, Fig. 3b, similar to the electron diffraction pattern in Fig. 2, with

six neighboring diffraction spots (4 of them of the 111 type and 2 of them of the 002 type). Because of the wavy aspect of {111} fringes, the 111 spots in the diffraction pattern are strong only in perfectly ordered regions where {111} fringes are perfectly defined. Therefore, it is possible to sort perfectly ordered regions and disordered or poorly ordered ones in the following basic way: A Fourier transform of the image is obtained and then filtered in order to eliminate the diffraction spots line resulting from these fringes. A reverse Fourier transform is performed and a smoothing treatment then provides various intensity levels which correspond to the different levels of ordering.

The main steps of the data treatment are summarized below:

(i) First, it can generally be observed that the photomicrograph background is not homogeneous at all; moreover, both arrays of white spots and fringes are blurred by some irregular noise. Therefore, this noise as well as various artifacts have to be removed from the data and the mean darkness of the image has to be made regular everywhere. At the end of this treatment the two different kinds of structures, black and white lines and white dots, can be distinguished more clearly on the image.

(ii) Second, the 2-D spectrum of the picture is obtained by mean of a fast Fourier transform (FFT). This transform is needed in order to separate the areas of the photomicrograph which exhibit white spots from those which exhibit fringes. The latter yield a linear spectrum of the  $0\ 0\ 2n$  diffraction spots, while the former provide a pseudosix-fold diffraction pattern (Fig. 3b) including the  $0\ 0\ 2n$  and the  $n\ n\ n$  and  $n\ n\ \bar{n}$  type diffraction spots. The whole line of  $0\ 0\ 2n$  spots in the reciprocal space is eliminated (Figs. 3c,d) in order to remove the fringe pattern from the image in the direct space. The background of the diffraction pattern is also reduced to zero. In this way, the Fourier transform of the image is cleansed of all information that is not relevant to the domain ordering.

(iii) Third, a reverse FFT is carried out in order to return from the Fourier space back to the direct space. As a result of the treatment only the arrays of white dots, although somewhat modified, are still visible. Indeed some information about these dots in the original image was lost during the data treatment, but fringes and dots regions now are clearly separated. No more information exists about the regions which previously exhibited fringes, these regions appear to be completely white, while regions containing spots appear to be more or less dark, relatively to the intensity of the  $n\ n\ n$  diffraction spots in the considered area.

(iv) A last smoothing treatment is necessary to erase the final contrast related to the former HREM image. Finally, an intensity histogram (3-D map) with 10 levels is obtained (Fig. 3e.) These levels correspond to the energy which is received in each point of the image. White

areas correspond to completely disordered regions (black and white fringes in the image), while black areas correspond to totally ordered regions (white spots in the image). The 8 other different levels correspond to intermediary "more or less ordered regions." The physical meaning of "more or less ordered regions" will be discussed later.

## TEST EXPERIMENT

An extensive study of the ordering of PST was already carried out (9, 10). Planar interfaces parallel to a {111} or to the (001) plane directions between a perfectly ordered region and a disordered one were shown to occur. Hence, we achieved a test experiment on a high resolution image of PST which clearly exhibits ordered and disordered regions (Fig. 3a). After computation (Fig. 3e) regions of different intensities on the intensity histogram (3-D map) are labeled from 0 (white) to 10 (black). The extreme limit of the region where some ordering can be detected (indicated by line "b" in Fig. 3a) fits, Fig. 3e, with the line of the computed image between regions of intensities 0 and 1 (the interface is parallel a {111} plane direction, with a step of one row of white spots). However, it can be seen that the line between regions 3 and 4 (line "a" in Fig. 3a) very best fits with the limit between the perfectly ordered region (probably all through the crystal, labeled (A) and the disordered one (labeled (B)). Because of this excellent fit, line "a" will be taken as the standard of the limit between ordered and disordered regions. This standard will be extended to all cases including the most general case when the interface is not parallel to the electron beam or even not planar.

It must be noted that practically no difference is visible, to the naked eye, on the image between regions of intensities ranging from 4 to 10. Finally the 3-D map gives seven different levels of ordering (from "low" to "high" ordering) in regions where the eye gives no difference of information about the ordering. The existence of regions of "low ordering," as given by the computation from 4 to 7 for example, can have different origins:

(i) Existence of stacking faults of the ordering (anti-phase boundaries), with a glide vector containing a component perpendicular to the [110] axis. They would shift the lattice of white spots and locally reduce the intensity of the  $nnn$  diffraction spots, hence resulting in a reduction of the intensity of the 3-D map in the region of the defect. This would have been visible to the naked eye if the stacking fault is a plane containing the [110] axis, which is not the case of region A (Fig. 3a), but this would not have been seen easily to the naked eye if the stacking fault is not planar, or is a plane not parallel to the [110] axis.

(ii) An ordered region may be not ordered throughout the whole crystal. This would reduce the relative intensity of the  $nnn$  diffracted spots and hence the apparent order-

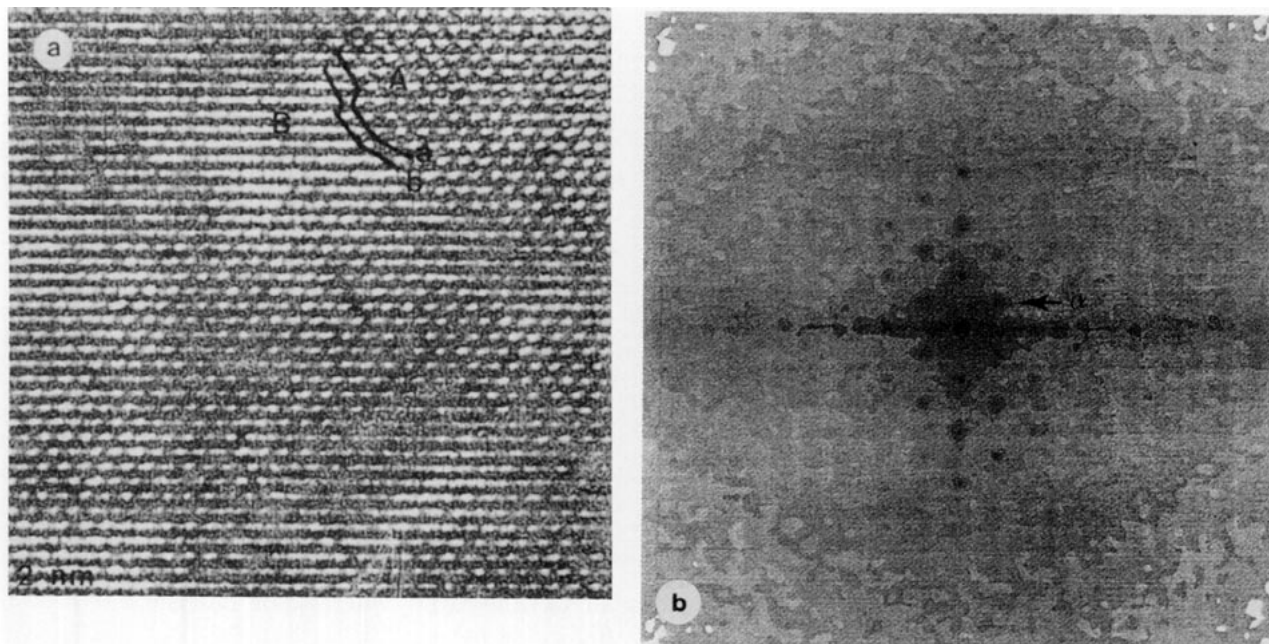


FIG. 3. (a) HREM images of PST used for the image computation test experiment. Line "a" corresponds to the limit between completely ordered (A) and at least partly disordered (B) regions, line "b" corresponds to the smallest possible ordering. (b) Fourier transform of (a). The strong vertical line of  $002n$  spots will be eliminated to eliminate fringes areas in the image. The background will also be eliminated. (c) Intensity along  $\alpha$  line (b) before filtration. (d) Intensity along  $\alpha$  line (b) after filtration. (e) Intensity histogram (3-D map) of the ordering of the image in (a). White regions are completely disordered regions and black regions are completely ordered regions. Line "a" which is the limit between ordered and disordered regions in (a) corresponds to the limit between regions of intensities 3 and 4. This limit will be taken as a standard between ordered and disordered regions in the next experiment. Line "b" is the limit between regions of intensities 0 and 1.

ing degree given by the 3-D map. This situation can occur in region A where ordering may not be present everywhere.

(iii) Ordering should be not perfect where it exists. Though this idea cannot be completely eliminated, it should be rather unlikely in the case of very small ordered domains and opportunities (i) and (ii) should, more likely, provide the existence of the "low ordering" areas.

Finally, some new information was obtained from an image that was expected to be perfectly known and which was used just as a standard.

#### USE OF THE COMPUTATION METHOD IN THE CASE OF PMN

When PMN is considered, HREM images are due to the superposition of black and white regular fringes parallel to the  $002$  plane direction with wavy fringes parallel to the  $(111)$  and  $(\bar{1}\bar{1}\bar{1})$  plane directions. This phenomenon yields a 2-D array of poorly ordered white dots. However, a careful scrutiny of the HREM images shows that perfectly ordered white-dot regions exist, separated by less ordered or disordered regions. The numerical treatment of the image that was previously tested is then used to determine

the boundary between ordered regions and disordered ones precisely.

The region which was selected for a numerical treatment is given in Fig. 4a and the result (a 3-D map of the intensity of ordering) is shown in Fig. 4b. Following the previous test experiment with the idea that ordered domains extend to the limit between levels 3 and 4 we can conclude that:

(i) Ordered regions, which appear black in Fig. 4b, are more or less circular. Most of them are about 2 nm in diameter, with a minimum of about 1.5 nm and a maximum of about 3 nm. The scattering of the size values is small.

(ii) Ordered domains as well as disordered regions are regularly spread out on the image. The regular array of ordered clusters is typical of PMN and is completely different from what occurs with PST for example.

As was previously indicated, the crystal is very thin (probably about 5 nm) in the regions where we get a good HREM image corresponding to the  $\langle 110 \rangle$  ZAP. The mean distance between the centers of neighboring ordered regions inside the crystal was obtained as follows: Ordered regions of the image which are so close to each other that they cannot be in the same plane are eliminated, then it is considered that the other regions are nearly in the same

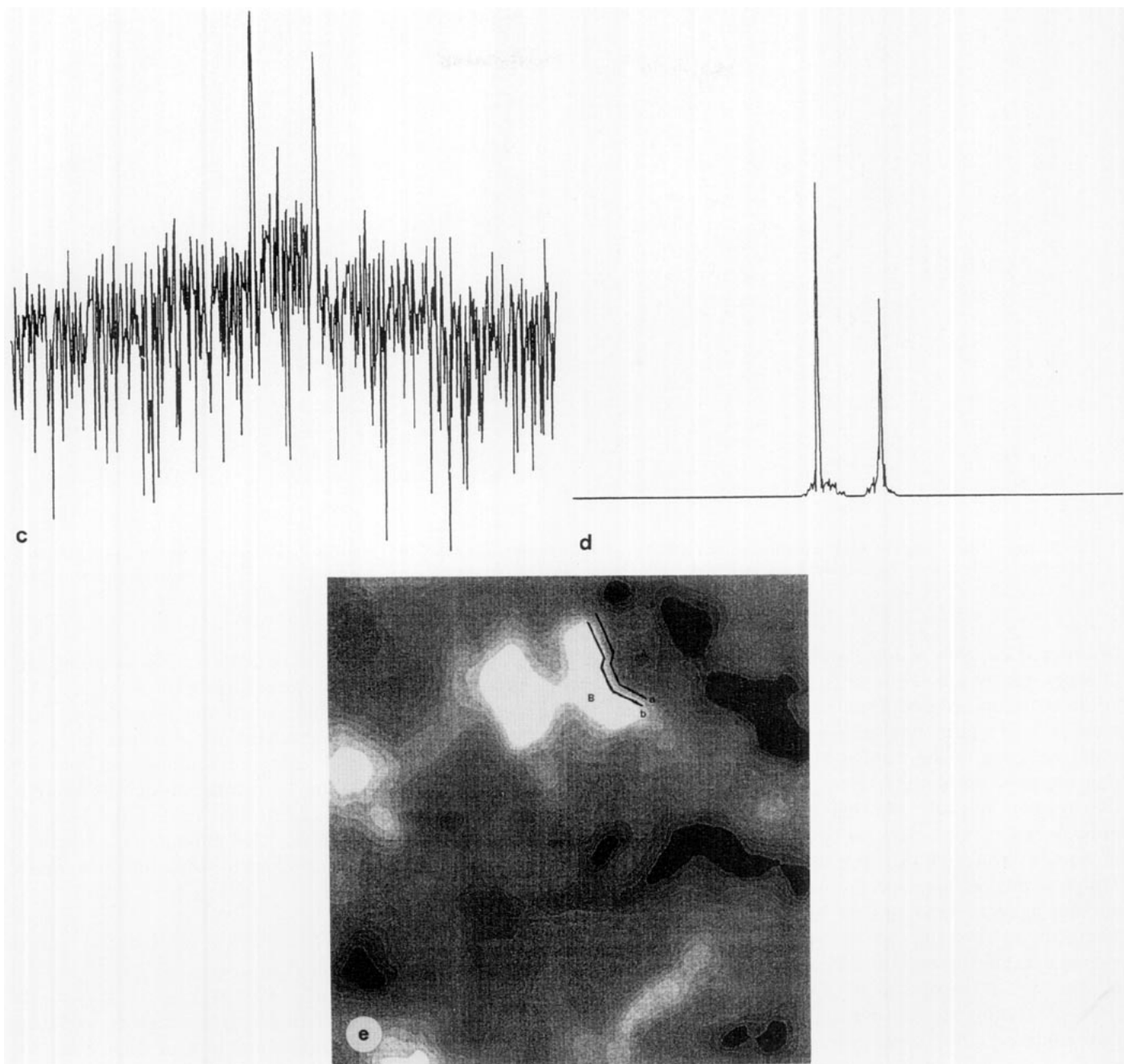


FIG. 3—Continued

plane and that the real distance in the crystal can be assimilated to the measured distance on the image. The latter distance is about 2.5 nm, so that the distance between the centers of two neighboring clusters is also 2.5 nm, with the following hypotheses: crystals are very thin, and clusters are nearly in the same plane. Nevertheless, because of the different hypotheses which were necessary, a rather important uncertainty on the experimental value must be accepted.

#### DISCUSSION

As previously suggested (7, 13–15) the composition of ordered domains of PMN is  $\text{PbMg}_{1/2}\text{Nb}_{1/2}\text{O}_3$  with a complete analogy of ordering with the other perovskites of this composition. For such a composition a local charge equilibrium does not exist so that only small ordered clusters can exist. The following facts that we have shown to occur: (1) existence of a regular array

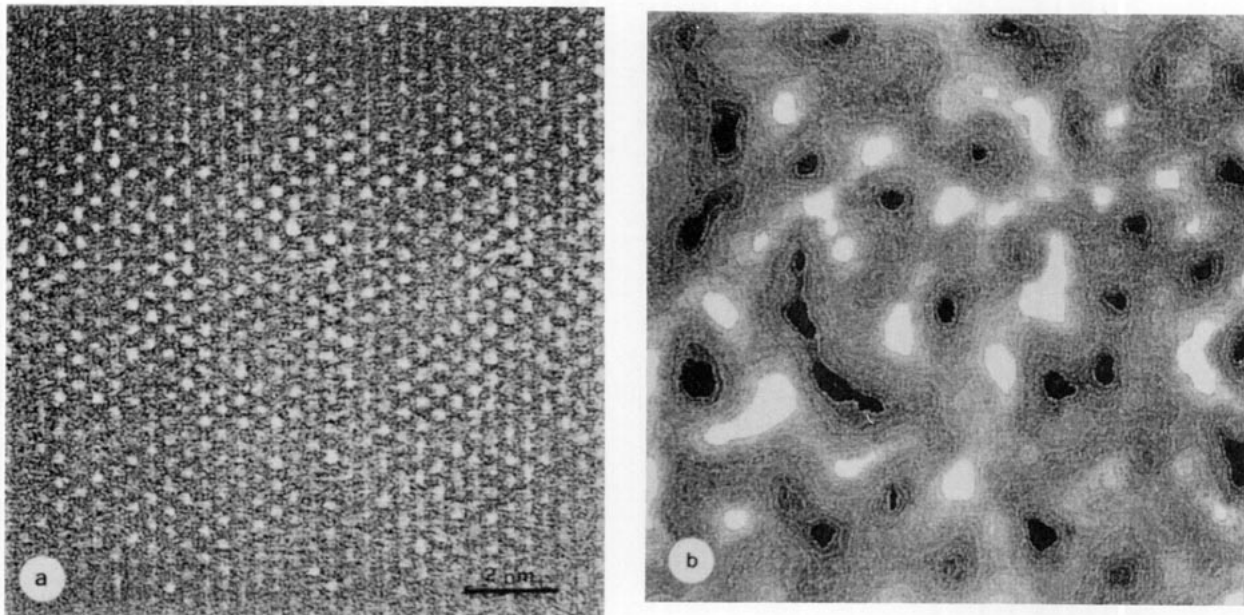


FIG. 4. (a) HREM image of PMN used for image computation. (b) Intensity histogram (3-D map) of the ordering of the image given in (a). White regions are disordered regions and black regions are ordered domains. The regular array of ordered and disordered regions is clearly visible.

of ordered clusters inside PMN. (ii) small size of these clusters, can be related to both the difference in composition between ordered and disordered domains and the local lack of charge equilibrium. On short distances the PMN ordering of the  $\text{PbMg}_{1/2}\text{Nb}_{1/2}\text{O}_3$  composition (Mg-rich clusters) certainly reduces the total free energy of the system, but the Mg-rich ordered clusters cannot grow over large distances for two reasons: the difference in composition and the lack of charge equilibrium. A Mg-poor region appears around each cluster so that another cluster cannot appear very close to its neighbor. Therefore, this results in the regular array of ordered clusters inside the crystal which is visible in projection in Fig. 4b. It is similar to the projection of a close packed stacking (a possible mixture of hexagonal and face centered cubic superstructures), but only a special study of this kind of stacking, using for example small-angle X-ray diffraction, could provide its precise characteristics. However, in the approximation of a clusters close packed structure, the mean distance between neighboring ordered clusters can be determined and is 2.5 nm and the diameter of the ordered clusters (supposed to be spherical) is 2 nm. Finally about  $\frac{1}{3}$  of the total volume is occupied by ordered clusters and  $\frac{2}{3}$  of the volume by disordered regions. The ordered regions composition being exactly  $\text{PbMg}_{1/2}\text{Nb}_{1/2}\text{O}_3$ , the composition of the disordered regions must be  $\text{PbMg}_{1/4}\text{Nb}_{3/4}\text{O}_3$ , to yield the mean  $\text{PbMg}_{1/3}\text{Nb}_{2/3}\text{O}_3$  composition. Because of the important uncertainty of the measurement of the

distance between the cluster centers, this composition is not determined with a large degree of accuracy. As the local charge equilibrium cannot occur inside ordered as well as inside disordered regions, the existence of oxygen vacancies inside ordered regions and that of metal vacancies (niobium or lead) inside disordered regions could compensate, at least partly, the lack of electrical charge equilibrium. This hypothesis, nevertheless, would have to be checked by some direct experimental method.

## CONCLUSIONS

The computation method that is used gives valuable information about localization and size of small ordered domains (less than 3 nm) when the dark-field image technique is no longer efficient.

In the case of PMN we have shown the existence of a regular array of ordered clusters. The shape of these clusters, their mean size and the mean distance between their centers were determined and the conclusion was that about  $\frac{1}{3}$  of the volume was ordered (with some degree of uncertainty). From these results the composition of disordered regions was deduced to be close to  $\text{PbMg}_{1/4}\text{Nb}_{3/4}\text{O}_3$ . Though a direct experimental determination should be useful to check all these results, we have got a quantitative description of the structural organization of the ordered PMN. The existence of atom vacancies was

proposed to solve, at least partly, the problem of the local lack of electrical charge equilibrium.

### REFERENCES

1. G. A. Smolenskii and A. I. Agranovskaya, *Sov. Phys. Solid State* **1**, 1429 (1959).
2. I. G. Ismailzade, *Sov. Phys. Crystallogr.* **5**, 292 (1961).
3. L. E. Cross, S. J. Jang, and R. E. Newnham, *Ferroelectrics* **2**, 183 (1980).
4. L. A. Shebanov, P. Kapostins, and J. Zvirgzds, *Ferroelectrics* **56**, 1057 (1984).
5. M. Lejeune, Thèse de Doctorat, Limoges, France, 1986.
6. D. K. Agrawal, R. Roy, and H. A. McKinstry, *Mat. Res. Bull.* **22**, 83 (1987).
7. E. Husson, M. Chubb, and A. Morell, *Mat. Res. Bul.* **23**, 357 (1988).
8. P. Bonneau, P. Garnier, E. Husson, and A. Morell, *Mat. Res. Bul.* **24**, 201 (1989).
9. N. Setter and L. E. Cross, *J. Appl. Phys.* **51**, 4356 (1980).
10. C. G. F. Stenger, F. L. Scholten, and A. J. Burggraaf, *Solid State Commun.* **32**, 989 (1979).
11. Z. C. Kang, C. Caranoni, I Siny, G. Nihoul, and C. Boulesteix, *J. Solid State Chem.* **87**, 308 (1990).
12. C. Caranoni, P. Lampin, I Siny, J. G. Zheng, Q. Li, Z. C. Kang, and C. Boulesteix, *Phys. Status Solid A* **130**, 25 (1992).
13. J. Chen, H. M. Chan and M. P. Harmer, *J. Am. Ceram. Soc.* **72**, 593 (1989).
14. A. D. Hilton, C. A. Randall, D. J. Barber, and T. R. Shrout, *Ferroelectrics* **93**, 379 (1989).
15. T. R. Shrout, W. Huebner, and C. A. Randall *J. Mater. Sci.* **25**, 3461 (1990).
16. H. M. Chan, M. P. Harmer, A. Bhalla, and L. E. Cross, *Jpn. J. Appl. Phys.* **24**(2), 550 (1985).
17. K. Z. Baba-Kishi and D. J. Barber, *J. Appl. Crystallogr.* **23**, 43 (1990).
18. G. Nihoul and M. H. Pishedda, *J. Solid State Chem.*, **105**, 469 (1993).